

# High-throughput random mutagenesis screen reveals TRPM8 residues specifically required for activation by menthol

Michael Bandell<sup>1,2</sup>, Adrienne E Dubin<sup>3</sup>, Matt J Petrus<sup>2</sup>, Anthony Orth<sup>2</sup>, Jayanti Mathur<sup>2</sup>, Sun Wook Hwang<sup>1,4</sup> & Ardem Patapoutian<sup>1,2</sup>

Menthol is a cooling compound derived from mint leaves and is extensively used as a flavoring chemical. Menthol activates transient receptor potential melastatin 8 (TRPM8), an ion channel also activated by cold, voltage and phosphatidylinositol-4,5-bisphosphate (PIP<sub>2</sub>). Here we investigated the mechanism by which menthol activates mouse TRPM8. Using a new high-throughput approach, we screened a random mutant library consisting of ~14,000 individual TRPM8 mutants for clones that are affected in their response to menthol while retaining channel function. We identified determinants of menthol sensitivity in two regions: putative transmembrane segment 2 (S2) and the C-terminal TRP domain. Analysis of these mutants indicated that activation by menthol involves a gating mechanism distinct and separable from gating by cold, voltage or PIP<sub>2</sub>. Notably, TRP domain mutations mainly attenuated menthol efficacy, suggesting that this domain influences events downstream of initial binding. In contrast, S2 mutations strongly shifted the concentration dependence of menthol activation, raising the possibility that S2 influences menthol binding.

Mint has been known for centuries for its ability to elicit a cool sensation. The active ingredient in mint that mediates this property is menthol, a cyclic monoterpene. Menthol activates TRPM8, a cold-sensitive ion channel of the TRP family<sup>1,2</sup>. Menthol is a member of a growing number of botanical compounds that modulate temperature-sensitive TRP channels (thermoTRPs). Heat-activated TRP vanilloid 1 (TRPV1) is activated by capsaicin, the active ingredient of chili peppers; noxious cold-activated TRP ankyrin 1 (TRPA1) is activated by pungent compounds such as cinnamaldehyde, mustard oil and garlic oil; and heat-activated TRPV3 and TRPV1 are activated by camphor<sup>3–9</sup>.

The mechanism of activation of thermoTRP channels by disparate chemical and physical stimuli is complex and mainly unknown. For example, TRPM8 is activated by cold temperature, compounds such as menthol and icilin (a synthetic compound), positive membrane potentials and the endogenous signaling lipid PIP<sub>2</sub> (refs. 10–13). These distinct stimuli seem to act on TRPM8 in a cooperative manner<sup>1,2,12,13</sup>.

Structural elements involved in transducing capsaicin and icilin stimuli have been elucidated. Capsaicin and icilin activate mammalian TRPV1 and TRPM8, respectively, but not their chicken orthologs. This has enabled structure-function studies using chimeras between avian and mammalian TRPV1 and TRPM8 to locate domains required for activation. For TRPV1, the linker region of transmembrane domains

2–3 (S2–S3) has been identified as a putative site for capsaicin binding<sup>14</sup>. In addition, intracellular domains of TRPV1 have been implicated in capsaicin sensitivity<sup>15</sup>. Analogous to the putative capsaicin binding site, residues in the S2–S3 linker region of TRPM8 are involved in icilin sensitivity but not in sensitivity to cold or menthol<sup>16</sup>. To date, residues required for menthol activation have not been identified. No species differences in menthol sensitivity have yet been identified for known TRPM8 orthologs, and chimeric proteins of TRPM8 and the menthol-insensitive TRPM2 (the closest homolog of TRPM8) have resulted in nonfunctional channels (data not shown). Here we used a new approach to identify structural elements involved in menthol sensitivity.

## RESULTS

### Identification of menthol-insensitive TRPM8 mutants

Using error-prone polymerase chain reaction (PCR), we randomly introduced mutations in the mouse *Trpm8* gene and created an extensive library of mutants. By screening the mutant library, we aimed to find mutants that were severely compromised in their sensitivity to menthol while retaining their sensitivity to cold.

TRPM8 sensitivity to cold and menthol was assayed using a fluorometric imaging plate reader (FLIPR), which measures changes in intracellular calcium levels in cells in a 384-well format. Sequential addition of cold saline buffer and 20 μM menthol yielded robust

<sup>1</sup>Department of Cell Biology, The Scripps Research Institute, La Jolla, California 92037, USA. <sup>2</sup>Genomics Institute of the Novartis Research Foundation, San Diego, California 92121, USA. <sup>3</sup>Department of Molecular Biology, The Scripps Research Institute, La Jolla, California 92037, USA. <sup>4</sup>Present address: Korea University Graduate School of Medicine, Seoul 136-705, Korea. Correspondence should be addressed to A.P. (ardem@scripps.edu).

Received 28 November 2005; accepted 14 February 2006; published online 5 March 2006; corrected 19 March 2006 (details online); doi:10.1038/nn1665

responses in cells transiently transfected with wild-type *Trpm8* but not in mock-transfected cells (Fig. 1a). Responses of TRPM8 to menthol were  $1.23 \pm 0.15$  (mean  $\pm$  s.d.) times larger than the responses to the cold buffer. Menthol exists in multiple stereoisomeric forms; unless specifically indicated, we used (-)-menthol for our studies.

A mutant library of  $\sim 14,000$  clones was screened; 31% of the clones responded to cold, menthol or both ( $\sim 4,300$  active clones). We focused on clones that showed severely deficient menthol responses but had cold responses that were  $> 35\%$  of those in the wild type—to ensure significant channel activity. Specifically, we selected 43 mutants whose menthol-to-cold response ratio was at least three times lower than that of the wild type (that is,  $> 5.4$  s.d. difference; see examples in Fig. 1a). Some clones were identified with the opposite profile (increase in menthol:cold response ratio); however, these mutants were less robust and proved to affect sensitivity to both menthol and cold (data not shown). Therefore, we focused on the menthol mutants.

Although the sequential addition of cold and menthol was convenient and sufficient for our primary screening purposes, the readout of the menthol responses was complicated by the fact that the cold buffer was still present at the time of menthol addition. We therefore tested the selected clones in a secondary FLIPR screen in which they were exposed separately to  $20 \mu\text{M}$  menthol or cold buffer. In 15 clones the menthol:cold ratio was at least three times lower than that in the wild type; these clones were sequenced. Five of these had ratios ten times lower than those in the wild type and became the focus of this study (Table 1). Subsequent site-directed mutagenesis showed that the loss of menthol sensitivity in these 5 clones could be accounted for by the substitution of Y745H, Y1005F or L1009R. Residues Y1005 and L1009 map to a C-terminal region called the TRP domain, a stretch of  $\sim 21$  residues that shows a high degree of conservation among TRP channels and is involved in  $\text{PIP}_2$  sensitivity<sup>11</sup> (Fig. 1). Residue Y745 maps to the middle of putative transmembrane segment 2 (S2). We

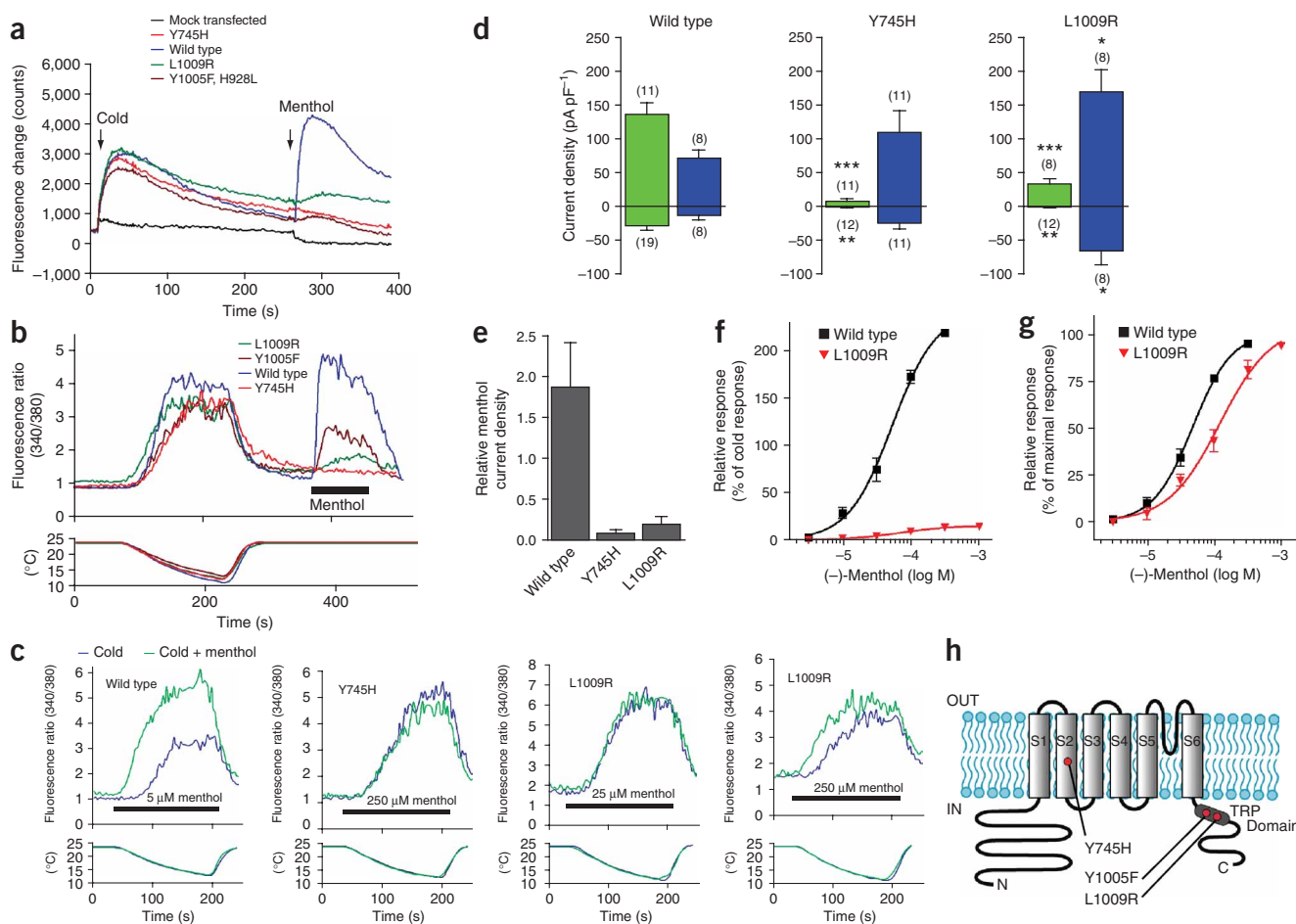


**Figure 1** Screening of a random mutant library identifies menthol-insensitive TRPM8 mutants. (a) FLIPR analysis of CHO cells expressing indicated channels. Cold buffer and  $20 \mu\text{M}$  menthol were added at the indicated times. (b) Ratiometric calcium imaging of CHO cells expressing indicated channels. Cells were exposed to gradual cooling (lower panel) and  $250 \mu\text{M}$  (-)-menthol (black bar, green trace) and second (after 150 s at  $24 \text{ }^\circ\text{C}$ ) in the presence of the indicated concentration of (-)-menthol (black bar, green trace). (c) Two consecutive cold responses are compared; first in the absence (blue trace) and second (after 150 s at  $24 \text{ }^\circ\text{C}$ ) in the presence of the indicated concentration of (-)-menthol (black bar, green trace). (d) Menthol ( $300 \mu\text{M}$ , green) and cold buffer ( $15\text{--}20 \text{ }^\circ\text{C}$ , blue) induced whole-cell current densities at  $-50 \text{ mV}$  (lower bars) and  $+80 \text{ mV}$  (upper bars) in HEK cells expressing indicated channels. The sensitivity of Y745H and L1009R to menthol was significantly lower than that of the wild type ( $**P < 0.001$  at  $-50 \text{ mV}$ ,  $***P < 0.0005$  at  $+80 \text{ mV}$ ;  $n$  is indicated). The response of Y745H to cold was not significantly different from that of the wild type, but the response of L1009R to cold was larger than that of the wild type ( $*P < 0.05$  at both  $-50 \text{ mV}$  and  $+80 \text{ mV}$ ), which might be accounted for by expression differences. (e) Menthol:cold current density ratio at  $+80 \text{ mV}$  as measured in d. Error bars account for propagation of uncertainties<sup>39</sup>. (f) Response as a function of (-)-menthol concentration for the wild type and for L1009R (measured at  $+50 \text{ mV}$ ). The response is expressed as a percentage of the cold response. Individual cells were normalized to the current obtained with  $300 \mu\text{M}$  of menthol. (g) As in f but the response is now expressed as a percentage of maximal menthol response. (h) Cartoon of the putative domain organization of TRPM8.

**Table 1 Mutations in clones lacking menthol sensitivity**

Mutant	Mutations				
1	T557S	Y924H	<b>L1009R</b>		
2	H818R	N1007T	<b>L1009R</b>	N1072S	Q1084R
3	<b>L1009R</b>				
4	H928L	<b>Y1005F</b>			
5	<b>Y745H</b>				

Bold indicates mutations that cause the phenotype when introduced as a single mutation.

sequenced the other ten clones and found that a mutation at position 1,013 in the TRP domain occurred in four of these clones (**Supplementary Table 1** online). Furthermore, an I846V mutation was observed in three clones. However, ratiometric calcium imaging experiments on cells transfected with TRPM8-I846V showed high internal calcium levels in the absence of any stimulus (data not shown). Thus, general channel function seemed to be significantly affected in this mutant.

To further characterize the Y745H, Y1005F and L1009R mutants, we performed ratiometric calcium imaging and analyzed the responsiveness of these mutants to a gradual cooling stimulus (cooling to  $\sim 12^\circ\text{C}$ ) and exposure to 250  $\mu\text{M}$  menthol, a concentration  $> 50$ -fold higher than the concentration that produces 50% of the maximum response ( $\text{EC}_{50}$ ) for the wild type (determined on FLIPR). Mutants Y745H, Y1005A and L1009R each responded to gradual cooling with response profiles similar to those of the wild type (**Fig. 1b**). We observed no response to 250  $\mu\text{M}$  menthol in Y745H, whereas there was a slight response in L1009R. The Y1005F mutant showed substantial activation by 250  $\mu\text{M}$  menthol. For further detailed analysis, we focused on Y745H and L1009R.

Subactivating concentrations of menthol potentiate the cold sensitivity of TRPM8 (refs. 1,2). Although menthol by itself elicited almost no or only slight activation of Y745H and L1009R, we considered the possibility that potentiation of the cold response by menthol might involve a distinct mechanism and may have been retained in these mutants. Therefore, we exposed cells expressing Y745H and L1009R to two sequential cold stimuli, first in the absence and then in the presence of menthol. The cold stimuli were given at intervals that did not cause tachyphylaxis (**Fig. 1c**). In both mutants, a low concentration of menthol (25  $\mu\text{M}$ ) did not potentiate the cold responses. At 250  $\mu\text{M}$ , menthol potentiated the cold response of L1009R, in agreement with this mutant being slightly menthol-sensitive, but not that of Y745H. We concluded that for both mutants, the decrease in potency to directly activate the channel parallels a decrease in potency to potentiate the cold response.

We next analyzed the sensitivity of these two mutants to cold and menthol using whole-cell patch-clamp experiments. TRPM8 is an outward rectifying channel by virtue of its voltage sensitivity<sup>12,13</sup>; in cells transfected with the wild type, Y745H or L1009R, small outward rectifying currents were observed at positive potentials. The application of cold or menthol to cells expressing wild-type TRPM8 elicited inward currents and increased the outward currents (**Fig. 1d** and **Supplementary Fig. 1** online). The currents generated by menthol were always larger than those evoked by cold. In contrast, only small menthol-induced currents were observed for Y745H or L1009R at high positive voltages, and these currents were only  $7.2 \pm 4.3\%$  and  $19 \pm 9\%$  of their respective cold-induced currents (versus  $188 \pm 54\%$  for the wild type) (**Fig. 1d,e**). The cold-induced response in L1009R was significantly larger ( $P < 0.05$ ) than that in the wild type. This may have been due to this mutant's hypersensitivity to cold. However, no such differences were observed in calcium imaging experiments. This difference can also be accounted for by enhanced channel expression in these cells

**Figure 2** Selective loss of menthol sensitivity by mutations in the S2 and TRP domains of TRPM8. **(a)** Voltage dependence of activation (derived from tail current analysis) of HEK cells expressing the wild type, Y745H or L1009R in the presence of 300  $\mu\text{M}$  menthol (green), at a cold temperature (blue,  $16\text{--}20^\circ\text{C}$ ) or in the absence of menthol at  $27^\circ\text{C}$  (black).  $V_{1/2}$  values are summarized in **Table 2**. **(b)** Rundown of voltage-activated TRPM8 in inside-out macropatches from *Xenopus* oocytes expressing the wild type, Y745H or L1009R channels. Time course of normalized currents after patch excision, measured at  $+120$  mV. Data were fit using a single exponential decay to determine rundown rates. A voltage ramp protocol from  $-80$  to  $+120$  mV was applied continuously at 1 Hz at room temperature ( $22\text{--}25^\circ\text{C}$ ). The membrane potential was held at 0 mV between sweeps. **(c)** Average rundown rates ( $\tau$ ) for the wild type ( $n = 7$ ), L1009R ( $n = 4$ ) and Y745H ( $n = 3$ ). **(d)** After current rundown (black trace), bath application of  $\text{diC8-PIP}_2$  (30  $\mu\text{M}$ ) increased outward currents (blue trace) in the wild type and in mutants. Patches were challenged with the indicated voltage ramps at  $15^\circ\text{C}$ . **(e)** Response as a function of the concentration of  $\text{diC8-PIP}_2$  (measured at  $+100$  mV,  $15^\circ\text{C}$ ) for the wild type ( $n = 2$ ), Y745H ( $n = 3$ ) and L1009R ( $n = 3$ ).

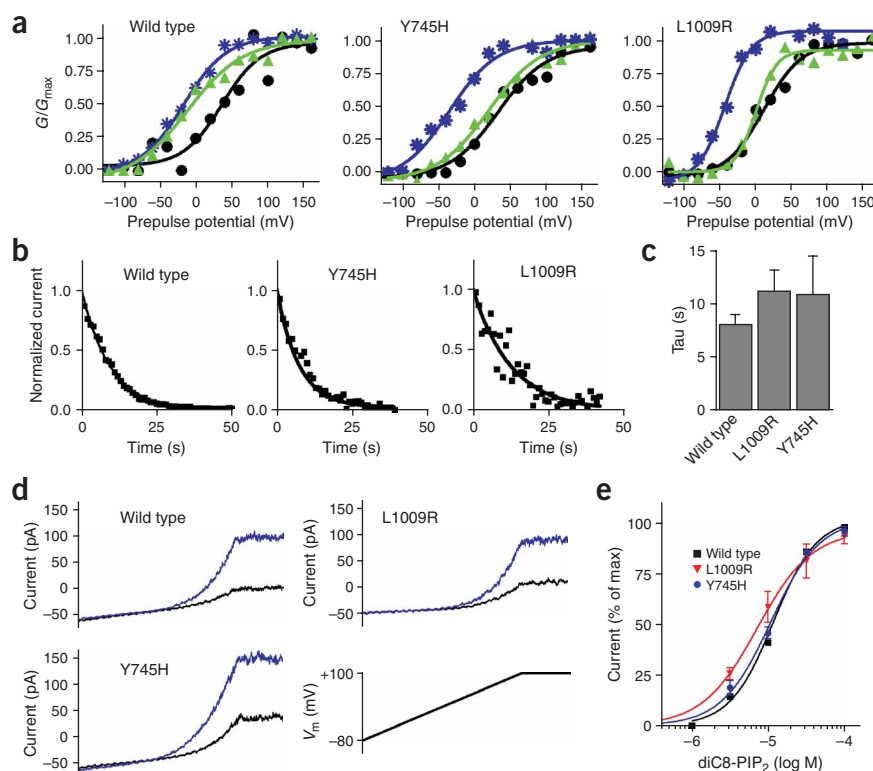


**Table 2**  $V_{1/2}$  values for wild-type TRPM8, Y745H and L1009R

	Wild type	Y745H	L1009R
Control	32 ± 8 (12)	35 ± 8 (7)	21 ± 4 (7)
Cool	-6 ± 7 (9)	-21 ± 9 (6)	-16 ± 4 (4)
Menthol	-31 ± 11 (8)	34 ± 6 (4)**	25 ± 6 (6)*

$V_{1/2}$  values (mV) obtained from tail analysis are shown as mean ± s.e.m. ( $n$ ).

\* $P < 0.005$ , \*\* $P < 0.0005$ . Control conditions: 26–28 °C. Cool conditions: 17–21 °C. Menthol conditions: 26–27 °C in the presence of 200–300  $\mu$ M menthol.

compared to the wild type (depolarization-activated outward currents at 26–29 °C in L1009R were 1.5 times those elicited in the wild-type). Although small, the currents in L1009R were sufficient to investigate the menthol concentration–response relationship. The  $EC_{50}$  for menthol was  $48 \pm 5 \mu$ M ( $n = 6$ ) for the wild type and  $122 \pm 32 \mu$ M ( $n = 4$ ) for L1009R (Fig. 1f,g). This difference was insufficient to account for the tenfold difference between the wild type and L1009R in relative menthol sensitivity (Fig. 1e,f). Thus the loss of menthol sensitivity was mostly due to a decrease in maximal response to menthol. Currents mediated by Y745H were too small to accurately determine  $EC_{50}$  values for menthol (but see below for analysis of Y745F).

### Specific loss of menthol sensitivity in Y745H and L1009R

Our initial results suggested that Y745H and L1009R mutations cause a loss in menthol sensitivity without a loss in cold sensitivity (schematic view of mutants' positions in Fig. 1h). Besides its cold sensitivity, TRPM8 is also known to be voltage-sensitive<sup>12,13</sup>. To further investigate whether Y745H and L1009R specifically affect menthol sensitivity, we asked whether voltage sensitivity had been changed. We therefore determined the voltage activation profile of Y745H and L1009R, and measured the voltage at which the conductance was half of its maximum ( $V_{1/2}$ ). The  $V_{1/2}$  values for these mutants were similar to those for the wild type (Fig. 2a and Table 2), indicating that the voltage sensitivity of these mutants was unaffected. Both cold and menthol shift the  $V_{1/2}$  to more negative values<sup>12,13</sup>. Given the allosteric interaction between voltage, menthol and cold, we asked whether menthol and cold were able to cause such a shift in our mutants. Cold temperature caused a shift in  $V_{1/2}$  in both mutants that was similar to the shift observed in the wild type. In contrast, the menthol-induced shift was severely attenuated in the mutants. These results indicated that voltage sensitivity in these mutants was unaffected and that cold sensitivity was similar to that in the wild type.

TRPM8 has recently been shown to depend on the presence of  $PIP_2$  (refs. 10,11). Dissociation of  $PIP_2$  from TRPM8 results in run-down of channel activity upon patch excision. Three positively charged residues in the TRP domain (K995, R998, R1008) have been implicated in  $PIP_2$  binding. We were intrigued that two-thirds of the isolated mutants had amino acid substitutions close to residues implicated in  $PIP_2$  sensitivity. We therefore

tested the hypothesis that these mutations indirectly attenuate menthol sensitivity by modification of the  $PIP_2$  dependence of the channel. To do this, we expressed the wild type, Y745H and L1009R in *Xenopus laevis* oocytes. We analyzed the rundown rate after patch excision, which is generally used as a measure of  $PIP_2$  affinity<sup>10,17</sup>. We assayed channel function using voltage ramps to +120 mV; these revealed currents in oocytes injected with the wild type and mutant cRNAs but not in water-injected eggs. After patch excision, the currents in both the wild type and the mutants were observed to run down (Fig. 2b). We quantified the rate of current rundown and found similar values for the wild type, Y745H and L1009R (Fig. 2c). In addition, the application of the dioctanoyl (diC8) analog of  $PIP_2$  after rundown to the cytoplasmic side of the membrane reversed current rundown in oocytes expressing Y745H, L1009R and wild-type TRPM8 (Fig. 2d). We observed no effect of diC8- $PIP_2$  in control oocytes (data not shown). To quantify the  $PIP_2$  sensitivity of our mutants, we analyzed the  $PIP_2$  responses over a range of concentrations (Fig. 2e). The resulting  $EC_{50}$  values for Y745H ( $11 \pm 1 \mu$ M;  $n = 3$ ) and L1009R ( $7 \pm 2 \mu$ M;  $n = 3$ ) were similar to that for the wild type ( $11 \pm 3 \mu$ M;  $n = 2$ ).

### Structural requirements for menthol sensitivity

All the mutants identified in our screen suggest that hydrophobic amino acid side chains have a key part in menthol sensitivity. An important role for hydrophobic elements in menthol sensitivity could be expected, given the hydrophobic nature of menthol. Indeed, camphor, a structurally related compound that is a substrate for the *Pseudomonas putida* cytochrome p450cam, binds to a hydrophobic pocket with a tyrosine residue involved in forming a hydrogen bond with its oxygen<sup>18</sup>. Notably, two tyrosines were identified in our screen. To test whether the hydrophobic nature or hydrogen binding abilities of the Y745, Y1005 and L1009 side chains were important, we substituted

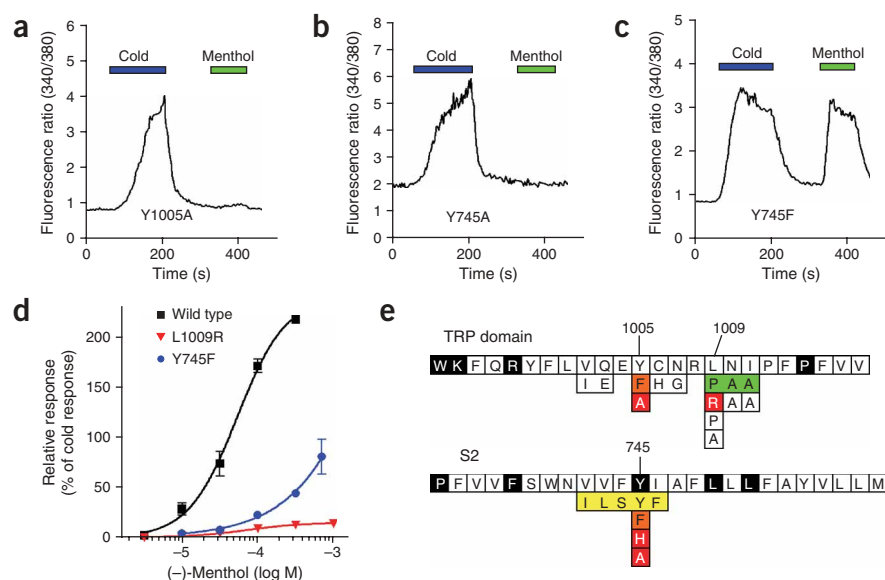


**Figure 3** Structural requirements for menthol sensitivity. (a–c) Ratiometric calcium imaging in CHO cells expressing the indicated mutants. Cells were exposed to cooling and 250  $\mu$ M menthol during the indicated times. (d) Response versus menthol concentration for Y745F, L1009R and the wild type. Whole-cell currents in individual cells were normalized to the response obtained with 300  $\mu$ M menthol and are expressed as a percentage of the cold response. (e) Summary of mutagenesis results. Top, mTRPM8 sequence of TRP domain and S2. Bottom, mutations in these domains. Black, conserved residue among the TRPM subfamily. Red, selective loss of menthol sensitivity. Orange, selective decrease of menthol sensitivity. Yellow, low responses to both cold and 250  $\mu$ M menthol. Green, change in ligand selectivity. White, no effect observed.

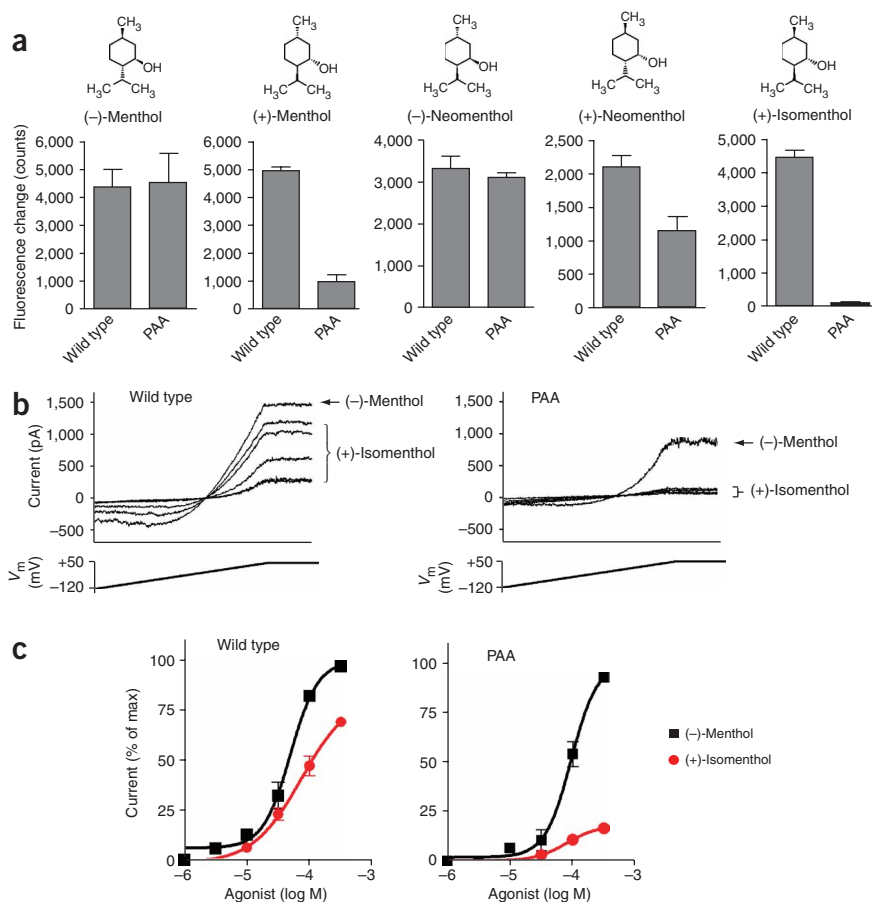


**Figure 4** Mutation of a tripeptide in the TRP domain alters ligand selectivity. **(a)** Intracellular calcium responses measured using FLIPR to 500 μM of the indicated menthol stereoisomers for CHO cells transfected with the wild type or LNI1009PAA (PAA). **(b)** Effect of (+)-isomenthol on the wild type and the LNI1009PAA mutant. Whole-cell currents elicited during ramps from -120 mV to +50 mV are shown. The current was sustained at +50 mV for 100 ms. Currents induced by voltage ramp are shown before and after the sequential application of increasing concentrations of (+)-isomenthol (0, 10, 30, 100 and 300 μM), after which 300 μM (-)-menthol was added (indicated). Currents reached steady state before the application of the next concentration. At the lowest concentrations, currents were monitored for at least 4 min. **(c)** Dependence of the wild type and the LNI1009PAA mutant on concentrations of (-)-menthol and (+)-isomenthol. Currents in each cell were normalized to the response to 300 μM (-)-menthol and expressed as a percentage of maximal menthol response. EC<sub>50</sub> values for (+)-isomenthol were determined at 75 ± 21 μM (*n* = 3) for the wild type and at 82 ± 15 μM (*n* = 3) for LNI1009PAA. EC<sub>50</sub> for (-)-menthol was determined at 43 ± 5 μM (*n* = 7) for the wild type and at 97 ± 14 μM (*n* = 5) for LNI1009PAA.

by only a moderate shift in EC<sub>50</sub> and very low maximal responses to menthol (**Fig. 3d**).

TRPM2 (ref. 19) is the closest homolog of TRPM8 (42% identical residues) and is menthol-insensitive (data not shown). We

asked whether differences in the side chain at the identified 745, 1,005 and 1,009 positions could explain this difference in menthol sensitivity. Notably, the Y745 and Y1005 residues are conserved between TRPM8 and TRPM2, and changing L1009 into a proline such as that found in TRPM2 did not cause a loss of menthol sensitivity. Thus the absence of menthol sensitivity in TRPM2 was not caused by differences in amino acid sequence at any of the positions identified in the screen. To test if differences at positions in close proximity to 1,005, 1,009 and 745 could explain the differences between TRPM8 and TRPM2, we generated mini-chimeras introducing stretches of two to five amino acids from TRPM2 into the TRPM8 sequence (**Fig. 3e**). All of the mini-chimeras in the TRP regions still responded to menthol, in a manner similar to the response of the wild type. The chimera in which we introduced part of the S2 domain of TRPM2 into TRPM8 also showed responses to menthol, albeit much lower than those in the wild type. However, cold responses in this mutant were also affected, suggesting that this mutation may affect general function. These data indicated that structural elements outside the 745, 1,005 and 1,009 regions are involved in bringing about the menthol sensitivity of TRPM8. Furthermore, we introduced the S2 and TRP domain of TRPM8 into TRPM2 to test whether it would be possible to make TRPM2 a menthol-sensitive channel. However, we did not observe responses to menthol from these chimeras (data not shown).

#### A TRP domain mutation modulates menthol stereoselectivity

Subtle changes in the ligand interaction and/or gating domains of ion channels have the potential to alter ligand discrimination between closely related compounds<sup>20,21</sup>. With the S2 and TRP domains as

these residues with various other residues and compared their menthol sensitivity (**Fig. 3**). Site-directed mutagenesis showed that L1009A or L1009P (proline is the most prevalent residue at this position in other TRPM channels) did not substantially affect menthol sensitivity: these mutant channels still responded to a low concentration of menthol (10 μM, data not shown). This suggests that a leucine side chain at position 1,009 is not essential, whereas the introduction of an arginine side chain, as was found in most of the mutants isolated from the screen, is detrimental for menthol sensitivity. This would fit a hypothesis that the charged side group of an arginine disrupts a hydrophobic environment necessary for menthol sensitivity. At position 1,005, an alanine disrupted menthol sensitivity to an even larger extent than the phenylalanine isolated from the library, suggesting that both the aromatic character and the hydroxyl group are important for menthol sensitivity (**Fig. 3a**). Additional mutagenesis in the S2 region revealed that Y745A had a menthol-insensitive phenotype similar to that of Y745H isolated from the library. Y745F had a more moderate effect: it affected menthol responses at low concentrations but allowed menthol responses at high concentrations (**Fig. 3b,c**). This suggested that both the hydroxyl group and the aromatic character of the tyrosine at this position are important for menthol sensitivity.

The residual activity in Y745F allowed for a more detailed analysis of this mutant with respect to its dependence on menthol concentration. Y745F caused a dramatic shift in the concentration-response profile. The currents generated by menthol did not saturate in the range tested, suggesting an EC<sub>50</sub> that is dramatically higher than that observed for the wild type (**Fig. 3d**). These characteristics make Y745F distinct from L1009R as the loss of menthol sensitivity for L1009R was characterized

potential ligand interaction and/or gating sites, we asked whether changes in these regions might alter ligand discrimination between menthol stereoisomers. For each stereoisomer, wild-type and mutant constructs (all constructs summarized in Fig. 3e) were tested simultaneously in a single FLIPR experiment, allowing a direct comparison of the responses. One of the mutants screened (a mini-chimera in which the tripeptide LNI at positions 1,009, 1,010 and 1,011 was replaced by PAA (LNI1009PAA)), showed only very low responses to 500  $\mu$ M (+)-isomenthol. This was not due to a lower overall channel function as responses to (-)-menthol and (-)-neomenthol were similar to those in the wild type (Fig. 4a). Responses to (+)-menthol and (+)-neomenthol were moderately affected. The change in stereoselectivity was confirmed in whole-cell patch-clamp experiments. (-)-Menthol elicited large currents in both the wild type and LNI1009PAA; however, (+)-isomenthol sensitivity was severely affected in LNI1009PAA, although small currents were still visible at positive voltages (Fig. 4b). We analyzed the concentration-response relationships for (+)-isomenthol and (-)-menthol for both the wild type and LNI1009PAA; this confirmed the difference in stereoselectivity between LNI1009PAA and the wild type (Fig. 4c). Notably, we obtained similar EC<sub>50</sub> values for (+)-isomenthol for the wild type and LNI1009PAA (wild type:  $75 \pm 21 \mu$ M,  $n = 3$ ; LNI1009PAA:  $82 \pm 15 \mu$ M,  $n = 3$ ) and only twofold differences in EC<sub>50</sub> values for (-)-menthol (wild type:  $43 \pm 5$ ,  $n = 7$ ; LNI1009PAA:  $97 \pm 14 \mu$ M,  $n = 5$ ). Thus the low (+)-isomenthol responsiveness in LNI1009PAA is best explained by a decrease in the maximal current (efficacy). Mutants containing individual L1009P, N1010A or I1011A substitutions showed only subtle changes in ligand sensitivity, suggesting that all three residues contributed to the effect in the triple mutant (data not shown).

### Icilin sensitivity is affected by Y745H and L1009R

Icilin is a synthetic cooling compound known to activate TRPM8 and TRPA1 (refs. 2,22). It is proposed that icilin acts through a mechanism

distinct from menthol, as icilin activation is strictly dependent on the presence of extracellular calcium<sup>16</sup>. We tested the sensitivity of the Y745H and L1009R mutants to 15  $\mu$ M icilin, a concentration 75-fold the EC<sub>50</sub> as determined on FLIPR (ref. 23). We were surprised to find that icilin was no longer able to activate these mutants (Fig. 5a–c). We proceeded to test the effect of icilin on LNI1009PAA. Icilin responses were severely attenuated, although some residual icilin response remained at 15  $\mu$ M (Fig. 5d). Icilin was unable to sensitize the Y745H and L1009R mutants to cold temperatures (Fig. 5e,f). In contrast, it retained its ability to markedly potentiate the cold responses of LNI1009PAA (Fig. 5g). These data showed that in spite of a differential need for cofactors, icilin and menthol sensitivity depend on common structural elements in the S2 and TRP domains.

### DISCUSSION

Mutagenesis studies have proved to be instrumental in obtaining new insight into the mechanisms of ion channel activation (for example see refs. 14,20,21,24,25). However, the process of generating and analyzing individual mutant channels is laborious, and the design of these mutations is often driven by preconceptions focusing on particular regions of ion channels. Here we described a new high-throughput random mutagenesis screen to identify residues required for the modulation of ion channels or receptors, without bias. The only requirements were (i) the availability of a fluorometric assay for channel or receptor function and (ii) the availability of two activating stimuli. Such experiments can be expected to yield insights into the functional elements of ion channels or G protein-coupled receptors (GPCRs) that are hard to obtain using other mutagenesis methods. Although we screened for a loss of agonist sensitivity, this methodology would be equally useful in screening for a loss of inhibitor sensitivity and could thus identify structural elements involved in inhibition.

A theoretical estimate suggested that, on average, each residue was substituted 10.5 times in our library (Supplementary Methods online).

The actual number of mutations per residue might have been lower because of mutation hotspots that, if present, would cause an unequal distribution of mutations. Furthermore, our mutagenesis was PCR-based and introduced single base pair substitutions. Therefore, each codon could only be changed to a few other codons (and could not yield all 20 amino acids). Thus our screen was not a saturating screen but most residues should have been mutated multiple times. The identified mutations from our screen highlight the advantage of this methodology. The S2 region mutation was in a conserved residue (Y745), which is a tyrosine in all TRPM channels. In chimeric constructs, this residue would have remained a tyrosine, and its involvement in menthol sensitivity would have gone unnoticed. One of the TRP domain mutations was at residue 1,009. Follow-up work on this residue showed that whereas an arginine had a dramatic effect on menthol sensitivity, several other residues did not. Both these examples highlight the power of an unbiased search using the random mutagenesis approach.

Our results showed that structural changes in the S2 and TRP domains can severely affect the sensitivity of the channel to menthol (and

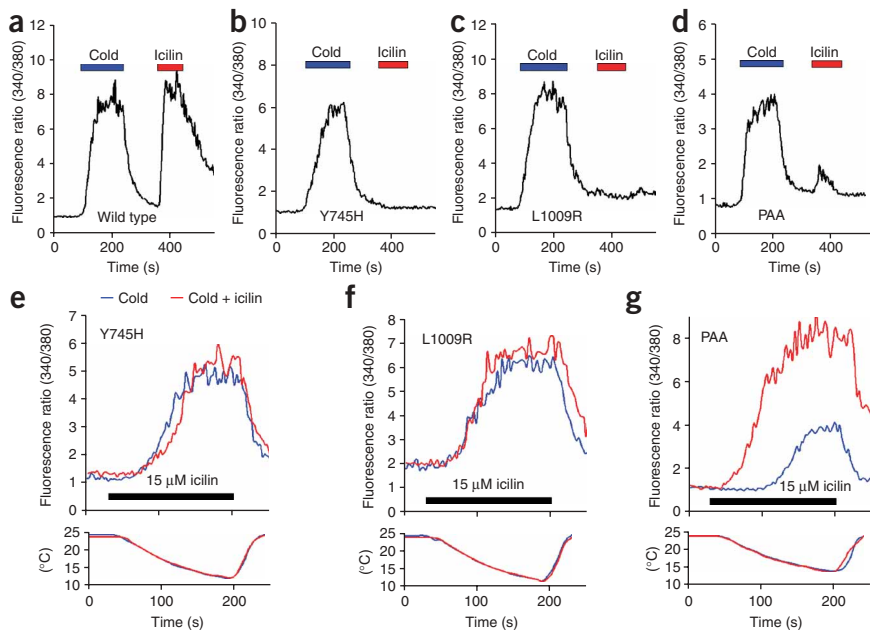


**Figure 5** Icilin sensitivity is lost in Y745H and L1009R. (a–d) Ratiometric calcium imaging of CHO cells transfected with indicated mutants using cooling stimuli (blue) and 15  $\mu$ M icilin (red). (e–g) Two consecutive cold responses are compared: first in the absence of icilin (blue) and second (after 150 s at 24 °C) in the presence of icilin (15  $\mu$ M, black bar, red trace). Traces of the two cold responses are overlaid for comparison.

icilin). Notably, three lines of evidence suggested that this effect is specific and is not paralleled by a general loss in channel function. First, the voltage dependence of the Y745H and L1009R channels was similar to that of the wild type. Second, the temperature activation profile of the mutant channels was comparable to that of the wild type, and cold temperature caused  $V_{1/2}$  shifts similar to those observed for the wild type. Third, the PIP<sub>2</sub> sensitivity of the mutant and wild-type channels was similar. Thus our data suggested that in the un-liganded state, these channels are not markedly different from the wild type in their ability to undergo the allosteric conformational changes required for channel opening.

How then can ligand-dependent activation be affected specifically? One possibility is that the mutations disrupted the ability of the channel to bind the ligand. Alternatively, the channel could be affected in its ability to translate ligand binding to channel opening (gating). For the TRP domain, our data support a model in which this region is involved in translating the initial ligand-binding event to the allosteric conformational changes that cause channel opening. This is supported by both the L1009R and LNI1009PAA mutants. Concentration-response profiles indicated that the low menthol responsiveness of these mutants was, to a large extent, caused by a decrease in the maximal response to menthol. The absence of dramatic changes in EC<sub>50</sub> suggested that the loss in menthol sensitivity is attributable to processes downstream of the initial binding event (including binding of menthol in the open state)<sup>20</sup>. We propose that the residues identified in the TRP region are required for coupling menthol binding to channel opening.

In addition to PIP<sub>2</sub> binding<sup>11</sup>, TRP domains have been implicated in protein-protein interactions. The TRP domain of TRPC1 binds Homer, an adapter protein that modulates channel function<sup>26</sup>, and the TRP domain of TRPV channels is thought to regulate oligomerization<sup>27</sup>. Our results suggest that this region is also involved in the ligand gating of TRPM8. The presence of a C-terminal gating domain bears a striking resemblance to what has been observed for cyclic nucleotide-gated (CNG) and hyperpolarization-activated cyclic nucleotide-gated (HCN) channels. CNG, HCN and TRP channels are part of the same large superfamily of ion channels that share structural similarities, including six putative transmembrane segments<sup>28</sup>. In CNG and HCN channels, a domain just C-terminal of S6, termed the C linker, has an important role in channel gating (for reviews see refs. 29–31). Alterations to the C linker influence ligand efficacy, analogous to the effects of the TRP domain mutations described here<sup>20,21,24,25,32</sup>. It will be interesting to test whether agonist sensitivity in other TRP channels also depends on this region. Notably, a T704A mutation in TRPV1, which corresponds to residue 1,001 of TRPM8 in alignments, dramatically reduces direct activation by phorbol 12-myristate 13-acetate (PMA)<sup>33</sup>. Additionally, a mutation juxtaposed to the TRP domain of the *Drosophila melanogaster* TRP channel results in only transient activity<sup>34</sup>.

The ligand-binding domain in CNG and HCN channels is located in the C terminus of the protein. In our experiments we found no evidence for a menthol-binding domain at the C terminus. Instead, we found evidence for the involvement of the S2 domain. The Y745H mutation caused a specific loss of menthol sensitivity and the Y745F mutation was associated with a dramatic shift in menthol EC<sub>50</sub>, suggesting a potential role of S2 in menthol binding. However, changes in EC<sub>50</sub> values for activity and binding assays can be caused by changes in the dissociation constant of the binding reaction and by changes in the equilibrium constant associated with channel opening<sup>35</sup>. At present, a cross-linkable menthol analog does not exist and thus the sites of contact with the channel have not been directly identified. Note that a

mutation in the S2 domain of TRPV1 (R491E) has been suggested to be involved in capsaicin binding<sup>14</sup>. The sequence homology between the S2 domains of TRPV1 and TRPM8 is very low, as is the structural similarity between menthol and capsaicin. However, these data suggest a common function for S2 in TRPV1 and TRPM8. Icilin is structurally distinct from menthol. Moreover, icilin requires calcium as a cofactor, whereas menthol does not. Icilin sensitivity depends on specific structural elements in the S2–S3 linker that were not required for menthol sensitivity<sup>16</sup>. In spite of these differences, we found that activation by icilin, like menthol, requires Y745 (and L1009), suggesting a commonality in their mechanisms.

How can the S2 and TRP domains work in concert to transduce menthol sensitivity? In a folded protein, these domains could be close to each other. The region just after 1,009 is hydrophobic, and the region upstream of 1,009 has been proposed to interact with PIP<sub>2</sub>, suggesting that the TRP region is tethered to the cytoplasmic side of the membrane. Thus, it is possible that the TRP domain interacts with the cytoplasmic side of S2. Ligand-induced structural changes of the S2 domain could couple to the pore via the TRP domain and stabilize the open state of the channel. However, the situation may be more complicated. For example, the crystal structures of distantly related voltage-gated potassium (Kv) channels show that the S2 domain is in close proximity to the S4 domain, which functions as a voltage sensor and couples to the pore<sup>36–38</sup>.

The mechanisms of TRP channel activation are complex and largely unknown. This is specifically true for thermoTRPs, which can be activated by a variety of physical and chemical stimuli. In this study, we focused on the identification of structural elements that are specifically required for the activation of TRPM8 by menthol but not by cold. At the onset of the study, it was not clear that such menthol-specific mutations existed. Indeed, it was entirely possible that TRPM8-gating was regulated by a single domain, responsible for coordinating the actions of voltage, cold and menthol<sup>12</sup>. However, the specific requirement of residues in the S2 and TRP regions clearly showed that this is not the case. Of course, the fact that some structural elements have a specific role in menthol activation does not exclude the possibility that other residues and domains might be involved in common roles of channel activation. Future studies will focus on elucidating what the other structural requirements are for TRPM8 activity and how these domains work in concert to explain the activation properties of TRPM8.

## METHODS

See **Supplementary Methods** online for further details.

**Mutagenesis screen.** We generated three mutant libraries in which the full-length and N- and C-terminal halves of TRPM8 were mutagenized using error-prone PCR (Diversify PCR random mutagenesis kit, Clontech)<sup>1</sup>. Plasmid DNA from about 4,000 transformants was isolated from each library.

Each cDNA from the mutant library was transfected in quadruplicate into Chinese hamster ovary (CHO) cells on 384-well assay plates. Two days after transfection, cells were loaded with Fluo-3 (Molecular Probes) and transferred to the FLIPR (Molecular Devices) to monitor fluorescence. Ice-cold assay buffer (25  $\mu$ l per well) was added, yielding a temperature decrease from 24 °C to ~17 °C. Cells were exposed to 20  $\mu$ M menthol 4 min after the cold addition.

**Ratiometric calcium imaging and electrophysiology.** Ratiometric calcium imaging (Fura-2 AM, Molecular Probes) were performed on transiently transfected CHO cells coexpressing yellow fluorescent protein (YFP)<sup>3</sup>. All calcium imaging graphs are averaged ratios of 20–40 individual cells. Conventional whole-cell patch-clamp experiments were performed on transiently transfected HEK293T cells coexpressing YFP. Extracellular solution: 124.5 mM NaCl, 2 mM MgCl<sub>2</sub>, 5 mM EGTA and 10 mM HEPES buffer (pH 7.4, with NaOH).

Pipette solution: 124.5 mM CsCl, 5 mM EGTA, 10 mM HEPES 10 and 1 mM MgATP (pH 7.4, with CsOH). Most experiments were performed at 26–29 °C unless otherwise indicated. Concentration dependence experiments were performed at 25 °C. Macrocurrents were recorded from inside-out patches from *Xenopus* oocytes injected with cRNA encoding the channels. Pipette (extracellular) solution: 96 mM NaCl, 2 mM KCl, 1 mM MgCl<sub>2</sub> and 5 mM HEPES (pH 7.4). Bath solution: 96 mM KCl, 5 mM EGTA and 10 mM HEPES (pH 7.4).

**Data analysis.** Data in all figures is shown as mean ± s.e.m. Statistical significance was evaluated using Student's *t*-test. Compound error analysis was used to determine the errors shown in **Figure 1e** (ref. 39).  $V_{1/2}$  determinations were obtained using the Boltzmann function to fit  $G/G_{\max}$  versus voltage curves derived from tail current analysis. The decay of the tail current at –120 mV was best fit by a single exponential.

*Note: Supplementary information is available on the Nature Neuroscience website.*

#### ACKNOWLEDGMENTS

We thank N. Gray, L. Miraglia, J. Zhang, M. Medina, A. Saghatelian, B. Cravatt, T. Jegla, V. Lee and S. Peters for valuable contributions and input. This work was supported by NINDS grant NS046303. M.B. is supported by a postdoctoral fellowship from the American Heart Association. A.P. is Damon Runyon Fellow and a member of the H. Dorris Neurological Research Institute.

#### COMPETING INTERESTS STATEMENT

The authors declare that they have no competing financial interests.

Published online at <http://www.nature.com/natureneuroscience>

Reprints and permissions information is available online at <http://npg.nature.com/reprintsandpermissions/>

- Peier, A.M. *et al.* A TRP channel that senses cold stimuli and menthol. *Cell* **108**, 705–715 (2002).
- McKemy, D.D., Neuhauser, W.M. & Julius, D. Identification of a cold receptor reveals a general role for TRP channels in thermosensation. *Nature* **416**, 52–58 (2002).
- Bandell, M. *et al.* Noxious cold ion channel TRPA1 is activated by pungent compounds and bradykinin. *Neuron* **41**, 849–857 (2004).
- Jordt, S.E. *et al.* Mustard oils and cannabinoids excite sensory nerve fibres through the TRP channel ANKTM1. *Nature* **427**, 260–265 (2004).
- Mogrich, A. *et al.* Impaired thermosensation in mice lacking TRPV3, a heat and camphor sensor in the skin. *Science* **307**, 1468–1472 (2005).
- Macpherson, L.J. *et al.* The pungency of garlic: activation of TRPA1 and TRPV1 in response to allicin. *Curr. Biol.* **15**, 929–934 (2005).
- Bautista, D.M. *et al.* Pungent products from garlic activate the sensory ion channel TRPA1. *Proc. Natl. Acad. Sci. USA* **102**, 12248–12252 (2005).
- Caterina, M.J. *et al.* The capsaicin receptor: a heat-activated ion channel in the pain pathway. *Nature* **389**, 816–824 (1997).
- Xu, H., Blair, N.T. & Clapham, D.E. Camphor activates and strongly desensitizes the transient receptor potential vanilloid subtype 1 channel in a vanilloid-independent mechanism. *J. Neurosci.* **25**, 8924–8937 (2005).
- Liu, B. & Qin, F. Functional control of cold- and menthol-sensitive TRPM8 ion channels by phosphatidylinositol 4,5-bisphosphate. *J. Neurosci.* **25**, 1674–1681 (2005).
- Rohacs, T., Lopes, C.M., Michailidis, I. & Logothetis, D.E. PI(4,5)P<sub>2</sub> regulates the activation and desensitization of TRPM8 channels through the TRP domain. *Nat. Neurosci.* **8**, 626–634 (2005).
- Voets, T. *et al.* The principle of temperature-dependent gating in cold- and heat-sensitive TRP channels. *Nature* **430**, 748–754 (2004).
- Brauchi, S., Orio, P. & Latorre, R. Clues to understanding cold sensation: thermodynamics and electrophysiological analysis of the cold receptor TRPM8. *Proc. Natl. Acad. Sci. USA* **101**, 15494–15499 (2004).
- Jordt, S.E. & Julius, D. Molecular basis for species-specific sensitivity to “hot” chili peppers. *Cell* **108**, 421–430 (2002).
- Jung, J. *et al.* Agonist recognition sites in the cytosolic tails of vanilloid receptor 1. *J. Biol. Chem.* **277**, 44448–44454 (2002).
- Chuang, H.H., Neuhauser, W.M. & Julius, D. The super-cooling agent icilin reveals a mechanism of coincidence detection by a temperature-sensitive TRP channel. *Neuron* **43**, 859–869 (2004).
- Zhang, H., He, C., Yan, X., Mirshahi, T. & Logothetis, D.E. Activation of inwardly rectifying K<sup>+</sup> channels by distinct PtdIns(4,5)P<sub>2</sub> interactions. *Nat. Cell Biol.* **1**, 183–188 (1999).
- Poulos, T.L., Finzel, B.C. & Howard, A.J. High-resolution crystal structure of cytochrome P450cam. *J. Mol. Biol.* **195**, 687–700 (1987).
- Nagamine, K. *et al.* Molecular cloning of a new putative Ca<sup>2+</sup> channel protein (TRPC7) highly expressed in brain. *Genomics* **54**, 124–131 (1998).
- Varnum, M.D., Black, K.D. & Zagotta, W.N. Molecular mechanism for ligand discrimination of cyclic nucleotide-gated channels. *Neuron* **15**, 619–625 (1995).
- Tibbs, G.R., Goulding, E.H. & Siegelbaum, S.A. Allosteric activation and tuning of ligand efficacy in cyclic-nucleotide-gated channels. *Nature* **386**, 612–615 (1997).
- Story, G.M. *et al.* ANKTM1, a TRP-like channel expressed in nociceptive neurons, is activated by cold temperatures. *Cell* **112**, 819–829 (2003).
- Behrendt, H.J., Germann, T., Gillen, C., Hatt, H. & Jostock, R. Characterization of the mouse cold-menthol receptor TRPM8 and vanilloid receptor type-1 VR1 using a fluorometric imaging plate reader (FLIPR) assay. *Br. J. Pharmacol.* **141**, 737–745 (2004).
- Zhou, L., Olivier, N.B., Yao, H., Young, E.C. & Siegelbaum, S.A. A conserved tripeptide in CNG and HCN channels regulates ligand gating by controlling C-terminal oligomerization. *Neuron* **44**, 823–834 (2004).
- Goulding, E.H., Tibbs, G.R. & Siegelbaum, S.A. Molecular mechanism of cyclic-nucleotide-gated channel activation. *Nature* **372**, 369–374 (1994).
- Yuan, J.P. *et al.* Homer binds TRPC family channels and is required for gating of TRPC1 by IP<sub>3</sub> receptors. *Cell* **114**, 777–789 (2003).
- Garcia-Sanz, N. *et al.* Identification of a tetramerization domain in the C terminus of the vanilloid receptor. *J. Neurosci.* **24**, 5307–5314 (2004).
- Yu, F.H. & Catterall, W.A. The VGL-chanome: a protein superfamily specialized for electrical signaling and ionic homeostasis. *Sci. STKE* **2004**, re15 (2004).
- Rosenbaum, T. & Gordon, S.E. Quickening the pace: looking into the heart of HCN channels. *Neuron* **42**, 193–196 (2004).
- Kaupp, U.B. & Seifert, R. Cyclic nucleotide-gated ion channels. *Physiol. Rev.* **82**, 769–824 (2002).
- Craven, K.B. & Zagotta, W.N. CNG and HCN channels: two peas, one pod. *Annu. Rev. Physiol.* **68**, 375–401 (2006).
- Johnson, J.P., Jr. & Zagotta, W.N. Rotational movement during cyclic nucleotide-gated channel opening. *Nature* **412**, 917–921 (2001).
- Bhave, G. *et al.* Protein kinase C phosphorylation sensitizes but does not activate the capsaicin receptor transient receptor potential vanilloid 1 (TRPV1). *Proc. Natl. Acad. Sci. USA* **100**, 12480–12485 (2003).
- Wang, T., Jiao, Y. & Montell, C. Dissecting independent channel and scaffolding roles of the *Drosophila* transient receptor potential channel. *J. Cell Biol.* **171**, 685–694 (2005).
- Colquhoun, D. Binding, gating, affinity and efficacy: the interpretation of structure-activity relationships for agonists and of the effects of mutating receptors. *Br. J. Pharmacol.* **125**, 924–947 (1998).
- Long, S.B., Campbell, E.B. & Mackinnon, R. Crystal structure of a mammalian voltage-dependent Shaker family K<sup>+</sup> channel. *Science* **309**, 897–903 (2005).
- Long, S.B., Campbell, E.B. & Mackinnon, R. Voltage sensor of Kv1.2: structural basis of electromechanical coupling. *Science* **309**, 903–908 (2005).
- Jiang, Y. *et al.* X-ray structure of a voltage-dependent K<sup>+</sup> channel. *Nature* **423**, 33–41 (2003).
- Taylor, J.R. *An Introduction to Error Analysis: the Study of Uncertainties in Physical Measurements.* (University Science Books, Mill Valley, California, 1982).